



# High-power transient 12–30 Hz beta event features as early biomarkers of Alzheimer's disease conversion: An MEG study

Danylyna Shpakivska-Bilan<sup>a,b</sup>, Gianluca Susi<sup>b,c</sup>, David W. Zhou<sup>d,e</sup>, Jesus Cabrera<sup>a,b</sup>, Blanca P. Carvajal<sup>a,b</sup>, Ernesto Pereda<sup>f</sup>, Maria Eugenia Lopez<sup>a,b</sup>, Ricardo Bruña<sup>b,g</sup>, Fernando Maestu<sup>a,b</sup>, Stephanie R. Jones<sup>d,e</sup>

<sup>a</sup>Department of Experimental Psychology, School of Psychology, Complutense University of Madrid, Madrid, Spain

<sup>b</sup>Center for Cognitive and Computational Neuroscience, Complutense University of Madrid, Madrid, Spain

<sup>c</sup>Department of Structure of Matter, Thermal Physics and Electronics, School of Physics, Complutense University of Madrid, Madrid, Spain

<sup>d</sup>Carney Institute for Brain Sciences, Brown University, Providence, RI, United States

<sup>e</sup>Department of Neuroscience, Brown University, Providence, RI, United States

<sup>f</sup>Department of Industrial Engineering and Institute of Biomedical Technology, Universidad de La Laguna, La Laguna, Tenerife, Spain

<sup>g</sup>Department of Radiology, Universidad Complutense de Madrid, Madrid, Spain

Corresponding Author: Danylyna Shpakivska-Bilan ([danyshpa@ucm.es](mailto:danyshpa@ucm.es))

## ABSTRACT

A typical pattern observed in M/EEG recordings of mild cognitive impairment (MCI) patients progressing to Alzheimer's disease (AD) is a continuous slowing of brain oscillatory activity. Definitions of oscillatory slowing are imprecise, as they average across time and frequency bands, masking the finer structure in the signal and potential reliable biomarkers of the disease progression. Recent studies show that high averaged band power can result from transient increases in power, termed "events" or "bursts." To better understand MEG oscillatory slowing in AD progression, we analyzed features of high-power oscillatory events and their relationship with cognitive decline. MEG resting-state oscillations were recorded in age-matched patients with MCI who later convert (CONV, N = 41) or do not convert (NOCONV, N = 44) to AD, in a period of 2.5 years. To distinguish future CONV from NOCONV, we characterized the rate, duration, frequency span, and power of transient high-power events in the alpha and beta band in two regions of interest in the "X" model of AD progression: anterior cingulate cortex (ACC) and precuneus (PC). Results revealed event-like patterns in resting-state power in both the alpha and beta bands, however, only beta-band features were predictive of conversion to AD, particularly in PC. Specifically, compared with NOCONV, CONV had a lower number of beta events, along with lower power events and a trend toward shorter duration events in PC ( $p < 0.05$ ). Beta event durations were also significantly shorter in ACC ( $p < 0.01$ ). Further, this reduced expression of beta events in CONV predicted lower values of mean relative beta power, increased probability of AD conversion, and poorer cognitive performance. Our work paves the way for reinterpreting M/EEG slowing and examining beta event features as a new biomarker along the AD continuum, and we discuss a potential link to theories of inhibitory control in neurodegeneration. These results may bring us closer to understanding the neural mechanisms of the disease that help guide new therapies.

**Keywords:** transient high-power events, magnetoencephalography, Alzheimer's Disease, computational neuroscience, mild cognitive impairment

Received: 20 September 2024 Revision: 12 May 2025 Accepted: 10 June 2025 Available Online: 25 June 2025



The MIT Press

© 2025 The Authors. Published under a Creative Commons Attribution 4.0 International (CC BY 4.0) license.

Imaging Neuroscience, Volume 3, 2025  
<https://doi.org/10.1162/IMAG.a.69>

## 1. INTRODUCTION

According to the [World Health Organization 2017](#), Alzheimer's disease (AD), a leading cause of disability and dependency among older individuals worldwide, is expected to affect 130 million people by 2050. Despite intensive research efforts, disease-modifying human therapies are still lacking, since the link between amyloid-induced cellular damage and cognitive decline is incomplete ([Maestú et al., 2021](#)). Magnetoencephalography (MEG) has been a valuable technique to fill this gap, as it can directly capture human neuronal processes, associated with the disease and cognition, with high temporal resolution ([da Silva, 2013](#); [Maestú et al., 2021](#)).

A typical pattern observed in M/EEG recordings of AD patients is a progressive slowing of brain oscillatory activity ([Dauwels et al., 2011](#); [Hsiao et al., 2013](#); [Ishii et al., 2017](#); [Jeong, 2004](#)), typically characterized by an increase in low-frequency delta (0.5–4 Hz) and theta rhythms (4–7 Hz), along with a decrease in higher frequency bands, alpha (8–12 Hz) and beta (12–30 Hz) rhythms. This oscillatory slowing initiates in early stages of the disease, such as mild cognitive impairment (MCI) ([Babiloni et al., 2004, 2009, 2010](#); [Dauwels et al., 2011](#); [Jelic et al., 2000](#)), and may even manifest before, in the subjective cognitive decline stage ([Bruña et al., 2023](#); [López-Sanz et al., 2016](#)), progressing from anterior to posterior cortices and particularly in frontal and parietal regions, ([Huang et al., 2000](#); [Nakamura et al., 2018](#)), in line with the onset of amyloid accumulation in the fronto-temporal association cortices ([Bang et al., 2015](#); [Cho et al., 2016](#); [Wiesman et al., 2022](#)). The “X” model of AD progression proposes that MCI patients who finally convert to AD exhibit a significant disruption (i.e., decrease in synchronization; [König et al., 2005](#); [López-Sanz et al., 2017](#); [Pusil, Dimitriadis, et al., 2019](#)) between anterior cingulate cortex (ACC) and precuneus (PC), two default mode network (DMN) hubs typically involved in the spreading of amyloid beta ([Forsberg et al., 2008](#); [Hampel et al., 2021](#); [Sepulcre et al., 2018](#)) and tau ([Hampel et al., 2021](#); [Tekin et al., 2001](#)) in the human cortex. As MEG oscillatory slowing accelerates, cognitive decline worsens producing alterations in memory processes and executive functions ([Hoshi et al., 2022](#); [Wiesman et al., 2022](#)).

Definitions of oscillatory slowing are imprecise, as they typically rely on methods based on a spectral decomposition followed by averaging across time, frequency bands, and often subjects. Such averaging can mask finer structure in the signal that may provide more reliable biomarkers of the disease progression and cognitive decline and help connect human biomarkers to the underlying neural mechanisms of the disease including possible connections to hyperexcitability as shown

in animal models ([Maestú et al., 2021](#); [Stoiljkovic et al., 2018](#); [Zott et al., 2019](#)). In recent years, there has been a shift in spectral M/EEG methods, as many studies have shown that, in non-averaged data, brain oscillations often occur as transient increases in high spectral power, a phenomenon termed oscillatory “bursts” or “events” ([Jones, 2016](#); [Lundqvist et al., 2024](#); [van Ede et al., 2018](#)). Quantifying transient changes in spectral activity requires new methods that consider temporal characteristics of spectral activity such as event rate, amplitude, duration, or frequency span ([Shin et al., 2017](#)). Such event-based methods have recently been applied in a growing body of M/EEG studies on the brain dynamics of cognitive processes ([Kavanaugh et al., 2023, 2024](#); [McKeon et al., 2023](#); [Morris et al., 2023](#); [Quinn et al., 2019](#); [Shin et al., 2017](#)), helping to establish neural correlates of cognitive behavior on a single trial level. Variability in oscillatory event parameters may represent a new set of explainable MEG biomarkers for AD progression, as it can reflect differences in circuit-level origins and provide insights into the underlying activity patterns and functions ([Jones, 2016](#); [Lundqvist et al., 2024](#); [M. A. Sherman et al., 2016](#)).

In this study, we applied standard power spectral density (PSD) and event-based analysis methods to resting-state MEG from adults with MCI who later convert (CONV) or do not convert (NOCONV) to AD. Motivated by the findings of the AD continuum model described by [Pusil, López, et al. \(2019\)](#) (namely the “X” model), we first hypothesized that averaged PSD slowing exhibits divergent effects in features of high-power transient spectral events. Second, we hypothesized that slowing-related effects in spectral event features would be associated with cognitive decline, as measured by a battery of neuropsychological tests in memory and executive functions in the MCI sample. We characterize MEG oscillatory slowing in terms of transient spectral event parameters in an MCI-to-AD longitudinal sample, taking the initial step toward the potential identification of biophysically principled biomarkers.

## 2. METHODS

### 2.1. Subject recruitment and neuropsychological assessment

Participants were recruited from Hospital Clínico Universitario San Carlos in Madrid, Spain. The study was approved by the ethics committee, and all participants provided written informed consent prior to participation. All participants were right-handed native Spanish speakers.

The study sample included 85 subjects diagnosed with mild cognitive impairment (MCI). At the first stage,

participants were screened according to the diagnostic criteria of the National Institute on Aging-Alzheimer's Association (NIA-AA) ([albert2011diagnosis](#)) and underwent a comprehensive neuropsychological assessment as previously described ([López et al., 2016](#); [Pusil, Dimitriadis, et al., 2019](#)), along with an MEG recording. At the second stage, in a temporal interval of 2.5 years, they

were subdivided in two groups considering the criteria for probable Alzheimer's disease ([McKhann et al., 2011](#)): 41 subjects with mild cognitive impairment who converted to AD (CONV), and 44 subjects with mild cognitive impairment (MCI) who did not convert to AD (NOCONV), see [Figure 1A](#). Subjects in the CONV and NOCONV groups were matched by age, sex, and education years, as it is

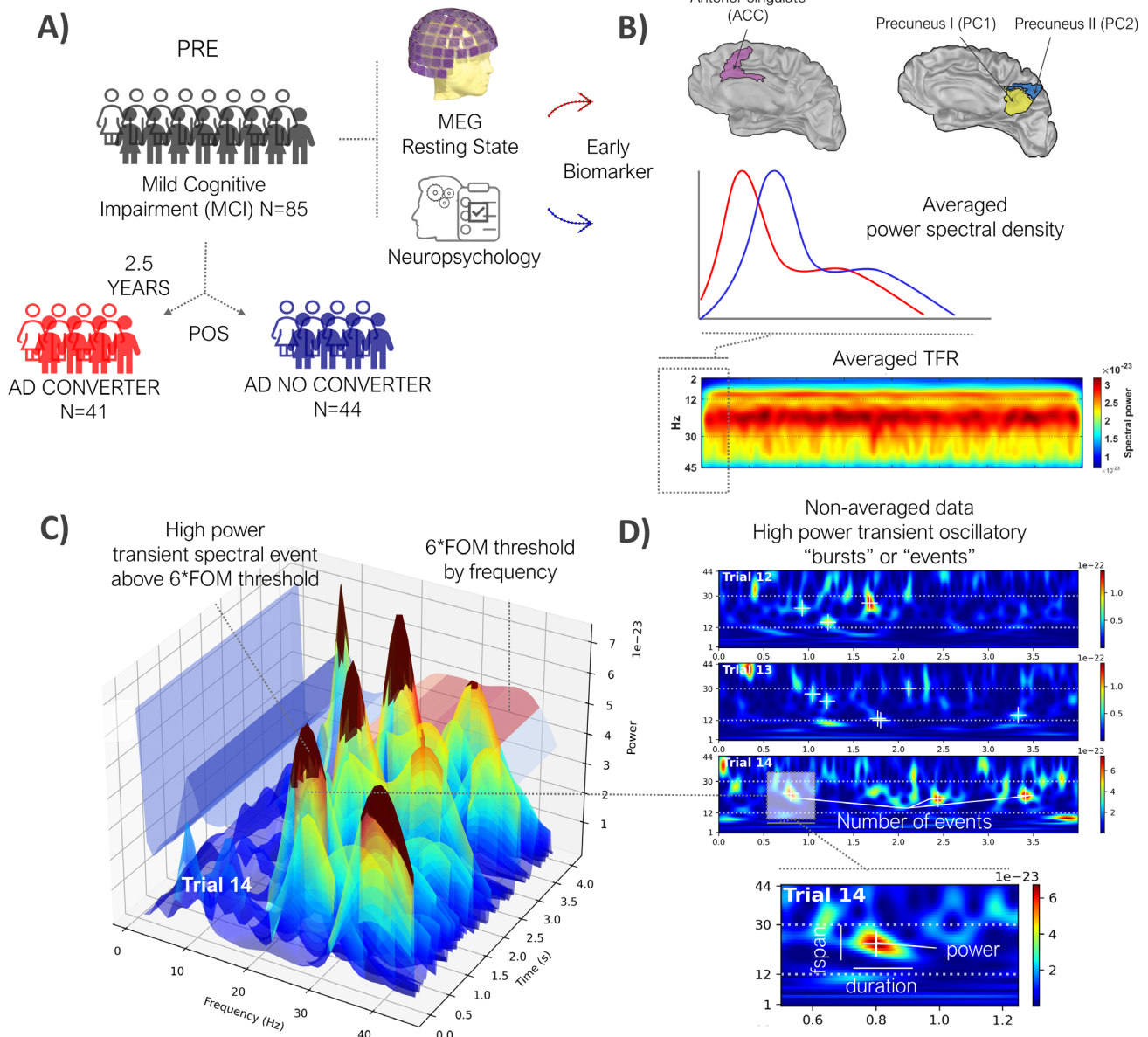


**Fig. 1.** (A) Illustration of the experimental design. Patients with mild cognitive impairment (MCI) were initially assessed using magnetoencephalography and neuropsychological testing. After 2.5 years, they were classified as Alzheimer's converters (CONV) or non-converters (NOCONV). (B) Averaged power spectra and time–frequency representations (TFR) were extracted from two regions of interest defined in the Schaefer 100-17 network atlas: *Sa/VentAttnB\_PFCmp\_1* (corresponding to ACC), *DefaultA\_pCunPCC\_1* (PC1), and *ContC\_pCun\_1* (PC2). (C) High-power transient bursts were detected as local maxima in the TFR exceeding a threshold of  $6 \times$  the factor-of-the-median (FOM) at each frequency, following [Shin et al. \(2017\)](#). (D) Example non-averaged TFRs from three resting-state segments in the left ACC. Several features of these events were extracted, as they may contribute to increases in average power across time and frequency, including event rate, duration, frequency span, and power.

**Table 1.** Mean  $\pm$  SD values of the demographic and neuropsychological characteristics for AD converters (CONV) and NOCONV groups.

Descriptives	NO CONV Mean $\pm$ SD	CONV Mean $\pm$ SD	p value
Age	75.25 $\pm$ 5.36	75.39 $\pm$ 4.99	t(83), p = n.s.
Sex	N = 44; 19 (m), 25 (f)	N = 41; 17 (m), 24 (f)	Xi (1), p = n.s.
Education years	9.89 $\pm$ 5.39	8.32 $\pm$ 4.30	t(71), p = n.s.
Immediate logic			
Memory units	17.30 $\pm$ 12.61	10.89 $\pm$ 7.41	t(83), p = 0.01
Delayed logic			
Memory units	7.64 $\pm$ 9.10	2.20 $\pm$ 4.08	t(83), p < 0.01
Immediate logic			
Memory themes	10.60 $\pm$ 5.03	7.70 $\pm$ 3.83	t(83), p < 0.01
Delayed logic			
Memory themes	4.86 $\pm$ 4.52	2.29 $\pm$ 2.47	t(83), p < 0.01
Inverse digits	4.16 $\pm$ 1.79	4.15 $\pm$ 1.28	t(83), p = n.s.
Semantic fluency	11.86 $\pm$ 3.56	11.15 $\pm$ 3.60	t(83), p = n.s.
Trail Making Test - B	211.15 $\pm$ 112.72	251.34 $\pm$ 108.15	t(83), p = n.s.
Boston Naming Test	46.45 $\pm$ 9.77	43.80 $\pm$ 8.74	t(83), p = n.s.
Clock-Drawing Test	5.43 $\pm$ 2.08	5.07 $\pm$ 2.26	t(83), p = n.s.

Non-significant p-values are marked as n.s.

reported in **Table 1** (data collected in stage 1, before division into NOCONV and CONV).

To be diagnosed with probable AD dementia, a patient must first meet the general criteria for dementia, which include cognitive or behavioral symptoms that interfere with daily activities, represent a decline from previous functioning, and are not explained by delirium or major psychiatric disorders. The onset of symptoms must be insidious, meaning they develop gradually over months to years. There must also be a clear history of cognitive decline reported by the patient or observed by others. Patients show an amnestic presentation (memory impairment) or language, visuospatial, or executive function deficits. Furthermore, the diagnosis of probable AD dementia should not be made if there is substantial concomitant cerebrovascular disease or other neurological conditions that could account for the cognitive decline.

The neuropsychological assessment included nine tests: four measures of memory recall, *Immediate Logic Memory Units*, *Delayed Logic Memory Units*, *Immediate Logic Memory Themes*, and *Delayed Logic Memory Themes* (Wechsler Memory Scale, WMS-III) (Wechsler, 1997); one measure of working memory, *Inverse Digits* (WMS-III); one measure of cognitive flexibility, *Trail Making Test-B* (TMT-B) (Bowie & Harvey, 2006); two language measures, *Semantic Fluency* (Controlled oral Word Association Test, COWAT) (Benton et al., 1994) and *Boston Naming Test* (BNT) (Kaplan et al., 1983); and one global screening measure for cognitive impairment and dementia, the *Clock-Drawing copy test* (Agrell & Dehlin, 1998). **Table 1** includes paired t-test and previously reported differences across groups (López-Sanz et al., 2016; Pusil, Dimitriadis, et al., 2019).

## 2.2. Magnetoencephalography data acquisition

The dataset was acquired using a 306-channel (102 magnetometers and 204 gradiometers) Vectorview MEG system (Elekta AB, Stockholm, Sweden) placed inside a magnetically shielded room (VacuumSchmelze GmbH, Hanau, Germany) located at the Laboratory of Cognitive and Computational Neuroscience (Madrid, Spain). MEG data consisted of 5 min eyes-closed resting-state recordings in a 60 min session, with a sampling rate of 1000 Hz and an online [0.1–330] Hz anti-alias band-pass filter. To allow further analysis, including subject-specific source reconstruction, MEG recordings were complemented by MRI scans acquired within a month after the MEG session, which were recorded at the Hospital Universitario Clínico San Carlos (Madrid, Spain) using a 1.5 T General Electric MRI scanner with a high-resolution antenna and a homogenization PURE filter (fast spoiled gradient echo sequence, with parameters: repetition time/echo time/inversion time = 11.2/4.2/450 ms; flip angle = 12°; slice thickness = 1 mm; 256  $\times$  256 matrix; field of view = 256 mm).

The MEG recordings were preprocessed offline using a temporal-spatial filtering algorithm (tSSS) (Taulu & Hari, 2009) (Maxfilter Software v2.2, correlation limit of 0.9 and correlation window of 10 s) to eliminate magnetic noises and compensate for head movements during the recording. The continuous MEG data were imported into MATLAB (R2017b, Mathworks, Inc.) for pre-processing steps, carried out using the Fieldtrip Toolbox (Oostenveld et al., 2011) (<https://www.fieldtriptoolbox.org/>). First, continuous data were automatically scanned for ocular, muscle, and jump artifacts using FieldTrip, with artifacts visually confirmed by an MEG expert (M.E.L.). Independent com-

ponent analysis (ICA) was then applied to remove the heart-related magnetic field artifact. Finally, the remaining artifact-free data were segmented into 4-s epochs. Source reconstruction was performed using minimum norm estimates (Hämäläinen & Ilmoniemi, 1994) with the software Brainstorm (Tadel et al., 2011) with current dipoles constrained to be perpendicular to the individual's cortical surface, to model the orientation of macro columns of pyramidal neurons (Tadel et al., 2011). Although MNE introduces spatial blurring, this approach allows for biologically meaningful inference of current flow direction along apical dendrites, which is essential for interpreting the results and guiding future computational modeling. To mitigate the depth bias inherent in minimum norm estimation, we applied lead field normalization, as implemented by default in the BrainStorm toolbox. Neural time series were finally averaged within regions of interest (ROI) of the Schaefer 100-17 network atlas (Schaefer et al., 2018). Two regions of interest were extracted for subsequent analysis: the anterior cingulate cortex (as the merge of *left ACC* and *right ACC*, corresponding to *SalV entAttnB PFCmp 1* area of the mentioned atlas, respectively), and the precuneus (as the merge of *left PC* and *right PC*, corresponding to *ContC pCun 1* and *DefaultA pCunPCC 1* area of the mentioned atlas), see Figure 1B. While our study focused on testing hypotheses in AC and PC based on prior studies, exploratory analysis of surrounding regions showed no significant differences in spectral event features (data not shown). The data were band-pass filtered between 0.5 and 45 Hz (broadband), using FIR filtering.

### 2.3. Power spectral density (PSD)

We computed the power spectral density of each of the ROI time series by using the Welch's periodogram method (Welch, 1967), with 1 s window length and 50% overlap ratio. For each ROI signal, the normalized power was calculated by averaging the power spectral density obtained by each epoch and then normalizing the value associated with each frequency by total power over the [1–30] Hz range.

### 2.4. Time–Frequency Representations (TFRs) & Spectral Events Extraction

During resting-state alpha and beta activities, periods of transient high power can be quantified over time in unaveraged data, see Figure 1B and D. We use a time-frequency-based algorithm as in Shin et al. (2017) to capture these bursts.

Time–frequency representations (TFRs) were calculated using the MATLAB SpectralEvents Toolbox (find

method = 1, as in Shin et al. (2017)) (<https://github.com/jonescompneurolab/SpectralEvents>). Each artifact-free 4-s epoch was convolved with a 7-cycle Morlet wavelet. For all epochs, TFR across time and across each patient was calculated and finally averaged to obtain a representative TFR for each ROI (PC or ACC) and group (CONV or NOCONV) in the range [2–30] Hz.

The bands of interest reflected the slowing effect typical of MCI (Bruña et al., 2023; Dauwels et al., 2011; López-Sanz et al., 2016) and observed in our sample and were chosen to be [5–10] Hz for alpha and [12–30] Hz for beta. (See also Methods Section 2.5 Statistical Analysis). More specifically, we defined alpha by determining the group averaged peak (GAP) frequency of 8 Hz in PC and taking a range of GAP [-3, +2] Hz. This choice provides a more precise capture of alpha oscillations in the aging population (Tröndle et al., 2023) and reflects the range of significant difference in both PC and ACC across groups in our sample (see Results Figure 2 below). The [12–30] Hz beta band, which does not exhibit a clear GAP, was similarly chosen to include the areas of significant difference in our sample.

Spectral Events were detected by first retrieving all local maxima in un-normalized TFR using *imregionalmax*. For each subject and ROI, transient high-power events were defined as local maxima above a  $6 \times$  factor of the median (FOM) threshold within a frequency band of interest, to be consistent with prior studies (Shin et al., 2017), see Figure 1C. The results computed with SpectralEvents remain largely unchanged after removing the aperiodic component (see Supplementary Figs. S2 and S3). To validate the robustness of our results, we also tested  $4 \times$  and  $8 \times$  FOM thresholds (see Supplementary Fig. S4; Supplementary Tables S1 and S2). As reported, we had the most significant results for  $6 \times$  FOM median threshold. The spectral event method applied (namely, find method = 1 in the SpectralEvent Toolbox) allows for multiple, overlapping events to occur in a given suprathreshold region and does not guarantee the presence of within-band, suprathreshold activity in any given trial, see Figure 1C and D.

Importantly, it was noticed that events detected in contralateral medial ROIs (especially in left ACC and right ACC) were in part mirrored across the midline due to the proximity of neighboring bilateral dipoles (this effect of spatial smearing in source reconstruction is explained in Supplementary Fig. S1). To remove duplicated mirror events when two detected events shared the corresponding contralateral ROI, epoch, time, and frequency, we rejected the one with lower amplitude.

For each subject and ROI, spectral events were characterized by four key features: event number in a fixed time window (i.e., event rate), duration, frequency span

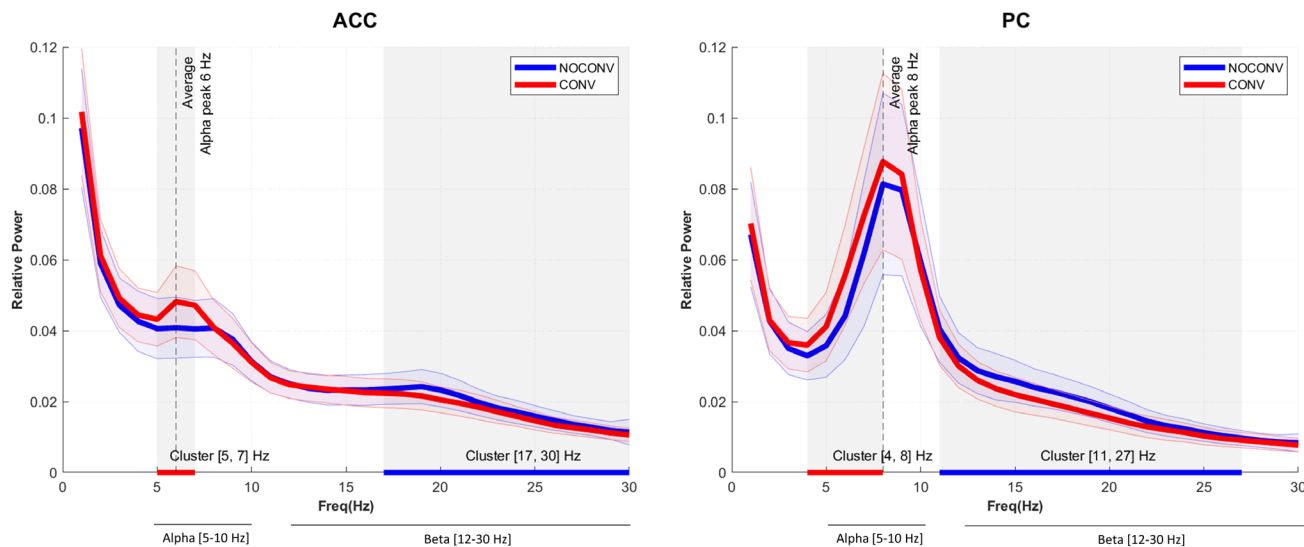


**Fig. 2.** Normalized power spectral density plots (mean  $\pm$  SEM) for regions of interest in CONV and NOCONV patients, in the range [2–30] Hz. Shaded gray areas represent statistically significant clusters of differences between CONV and NOCONV groups (non-parametric statistical test).

(Fspan), and power (Power FOM) (see Fig. 1D). Event number was calculated by counting the number of events in the 4-s period of each epoch. Event power was calculated as the normalized FOM power value at each event maximum. Event duration and frequency span were calculated from the boundaries of the region containing power values greater than half the local maxima power, as the full-width-at-half-maximum in the time and frequency domain, respectively.

## 2.5. Statistical analysis

To determine frequency ranges that represent oscillatory slowing in our cohort, we tested for significant differences in average power spectral density between AD CONV and NOCONV for each selected ROI by performing a non-parametric statistical test (Maris & Oostenveld, 2007) in the frequency domain (see light gray window in Fig. 2).

In each frequency band, we examined the relationship between event features and the averaged PSD using a linear regression analysis over all subjects. The regression  $\beta$  coefficients were calculated with a 95% CI and all  $p$ -values were corrected for multiple comparisons using the Benjamini–Hochberg (BH) step-up procedure (Benjamini & Hochberg, 1995) with a False Discovery Rate (Q) set at 0.05. Statistically significant  $p$ -values after BH correction are reported as  $^*p < 0.05$  ( $Q = 0.05$ ).

We also tested for group differences in spectral event features between CONV and NOCONV groups. High-power spectral event features were detected in alpha and beta frequency bands for each resting state segment from four ROI's (left and right ACC and PC, respectively).

Event rates were averaged across epochs, and other features (duration, f-span, power) were averaged across all events, and then between hemispheres, within each subject. The final dataset consisted of 16 variables for each subject: four event features (averaged spectral event rate, duration, f-span and power); by two ROI's (ACC, PC); by two frequency bands (alpha and beta). For each variable, t-tests were used to assess group differences in transient event features. To account for potential differences in variance between groups, we tested the assumption of homoscedasticity prior to applying statistical tests; when violated, we used MATLAB's `ttest2` function with the “`vartype`”, “`unequal`” option, which implements Satterthwaite’s approximation to address the Behrens-Fisher problem. The tests were conducted with a left tail for the beta band and a right tail for the alpha band. This approach was consistent with the observation that the average power spectra in the alpha band are higher for CONV compared to NOCONV, while the effect is reversed in the beta band. We hypothesized that differences in event features align with the directional trend observed in the averaged relative spectral power. All reported  $p$ -values were corrected for multiple comparisons across the number of tests applied using the Benjamini–Hochberg (BH) step-up procedure (Benjamini & Hochberg, 1995) with a False Discovery Rate (Q) set at 0.05. Statistically significant  $p$ -values after BH correction are reported as  $^{**}p < 0.05$  ( $Q = 0.05$ ). Statistical tendencies are reported as significant if  $*p < 0.1$ . We computed effect size of the differences between groups with a robust variant of Cohen’s  $d$  (Algina et al., 2005).

For event features where significant difference across groups were found, we examined the relationship

between these features and AD conversion and cognitive performance.

To assess the relationship with AD conversion, we fit beta event features from ACC and PC to a logistic regression model (R *glm()* function, *family = binomial* argument) to predict each patient's conversion label (CONV or NOCONV). The model's output is the probability of the positive class (CONV group). We used a default 0.5 threshold value to transform the probability to a binary class. Thus, a subject is classified as class 1 (CONV) if the predicted probability is greater than or equal to 0.5, and class 0 if the probability is less than 0.5. The odds ratio in logistic regression is calculated by exponentiating the coefficient of the predictor variable. As an example, for predictor variable *Number of events*, if the coefficient is  $\beta = 0.58$  the odds ratio is given by  $OR = e^{0.58} \approx 1.79$ . This means that the likelihood of the predicted outcome (AD conversion) is approximately 1.79 times greater than the likelihood of the outcome not occurring (no conversion to AD). Every reduction of 1 unit in *Number of events* increases by 79% the odds of AD conversion (CONV group).

To assess the relationship with cognitive performance, we calculated a Cognitive Performance Index and applied linear regression. Aiming to account for variability across the nine neuropsychological tests used, the Cognitive Performance Index was calculated by applying Principal Components Analysis (PCA) (R *princomp()* function) to the neuropsychological testing dataset. As a first step, the data from each of the nine tests were z-scored to prevent biases due to different test scales. Additionally, the data were transformed so that for each test, higher values correspond to better cognitive performance. Then, we extracted the first principal component, which explained at least 55% of variance. The projection of individual data onto the new axes (principal component) represents the Cognitive Performance Index values for each subject, and this projection is achieved through linear transformation using the eigenvectors of the covariance matrix. All eigenvectors had a positive load in the first component. A subject with higher values of this Cognitive Performance Index corresponds to better cognitive performance.

### 3. RESULTS

#### 3.1. AD converters (CONV) exhibit oscillatory slowing in average PSD

We confirm a slowing effect in power spectral density in CONV subjects for all ROIs of interest in ACC and PC, as observed in prior studies (Pusil, Dimitriadis, et al., 2019). In averaged PSD, the CONV group shows a statistically

significant cluster of decreased relative power in beta frequency band compared with NOCONV (Fig. 2; 17–30 Hz ACC and 11–27 Hz PC, blue underlines) and increased relative power in lower frequency bands (theta, low-alpha) (Fig. 2; 5–7 Hz ACC and 4–8 Hz PC, red underlines). Based on our data, for all subsequent analyses, we utilized a [5–10] Hz alpha bands and [12–30] Hz beta band (see Methods section 2.4 for further details).

#### 3.2. Resting-state alpha and beta emerge as transient high-power events

The PSD plots of Figure 2 rely on Fourier analysis performed on averaged epochs of brain activity from the two different groups. As described previously, differences in averaged power across patient groups could emerge from several features in transient of high-power activity (i.e., events) in the unaveraged data.

Visual inspection of time-frequency representations in Figure 3 shows that seemingly continuous high average power in the alpha and beta bands (top panels) is the result of the accumulation of transient high-power activity ("events") across epochs of the unaveraged resting-state data (Fig. 3, middle and bottom panels) for both groups.

As such, higher averaged power could be due to increased expression in several features, including a higher number of events (rate), longer duration events, increased frequency spans, and/or increased power of the event. To assess whether these features contributed to averaged power in our sample, we performed a regression analysis between each feature and averaged alpha and beta power (Fig. 4). Our results show a strong correlation with averaged power and each event features in the beta band (number:  $\beta = .28$ ,  $R^2 = .069$ ,  $p - value = .0088$ ; duration:  $\beta = .45$ ,  $R^2 = .192$ ,  $p - value < .0001$ ; max power:  $\beta = .41$ ,  $R^2 = .156$ ,  $p - value = .0001$ , frequency span:  $\beta = -.29$ ,  $R^2 = .07$ ,  $p - value = .0075$ ). While similar relationships occurred between alpha event features and averaged alpha power, only alpha event frequency span significantly correlated with averaged alpha power after correction for multiple comparisons and the effect was weaker than in the beta band (frequency span:  $\beta = -.25$ ,  $R^2 = .05$ ,  $p - value = .025$ ).

#### 3.3. Reduced beta event features as predictive biomarkers of AD conversion and cognitive decline

Given the event like nature of alpha and beta, we next tested the hypothesis that the slowing observed differences across groups in averaged PSD power in Figure 2 was due to across group differences in event features, namely rate, power, duration, and/or frequency span. We

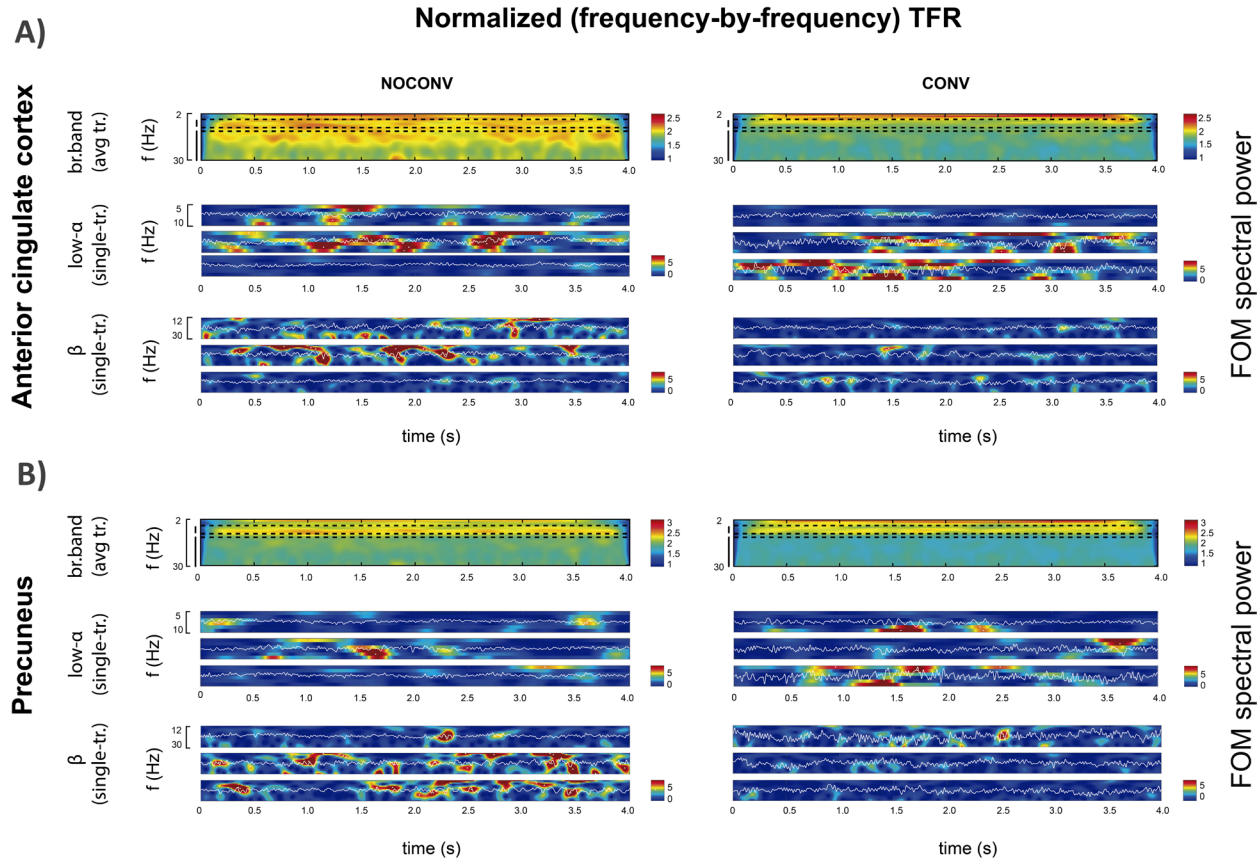


**Fig. 3.** Time–frequency representations of spectral events in PC (A), and ACC (B) for non-converters (NOCONV, left) and converters (CONV, right) groups. For each case, we show the representative averaged broadband TFR (top), as well as three TFR related to randomly chosen trials for low-alpha (middle), and beta (bottom) band.

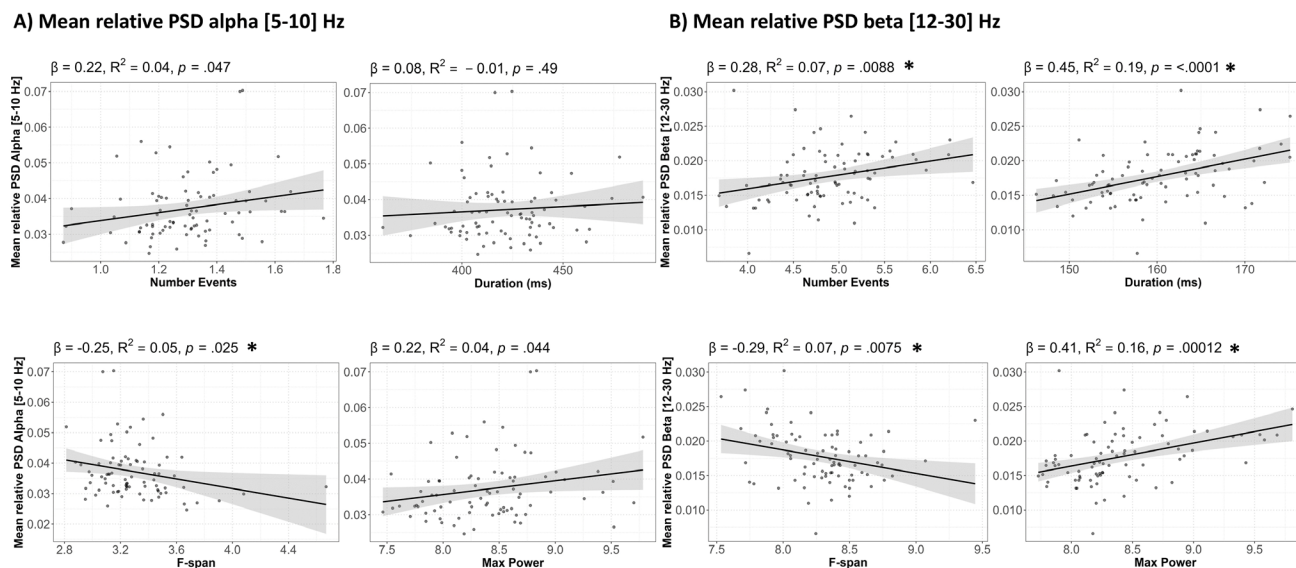


**Fig. 4.** Diminished expression of event features in ACC and PC is associated with reduced mean power spectral density (PSD). (A) Regression analysis between alpha [5–10] Hz spectral events and averaged alpha power. (B) Regression analysis between beta [12–30] Hz spectral events and averaged beta power. Statistically significant  $p$ -values after BH correction are reported as \* $p < 0.05$  ( $Q = 0.05$ ).

found effects only in the beta band that were more prominent in PC, such that CONV had a lower mean rate of beta events, lower power events, and a trend to shorter duration beta events in PC. Shorter duration beta events were also present in ACC in the CONV group (Fig. 5; Table 2; rate in PC  $p\text{-value}_{BH} = .003$ , power in PC

$p\text{-value}_{BH} = .002$ , duration in PC  $p\text{-value}_{BH} = .051$ ; duration in ACC  $p\text{-value}_{BH} = .01$ , see also Supplementary Figures S5 and S6 for further summary statistics). Notably, the effect size for differences between CONV and NOCONV in these features is of medium size ( $Cohend > 0.4$ ), see Table 2.

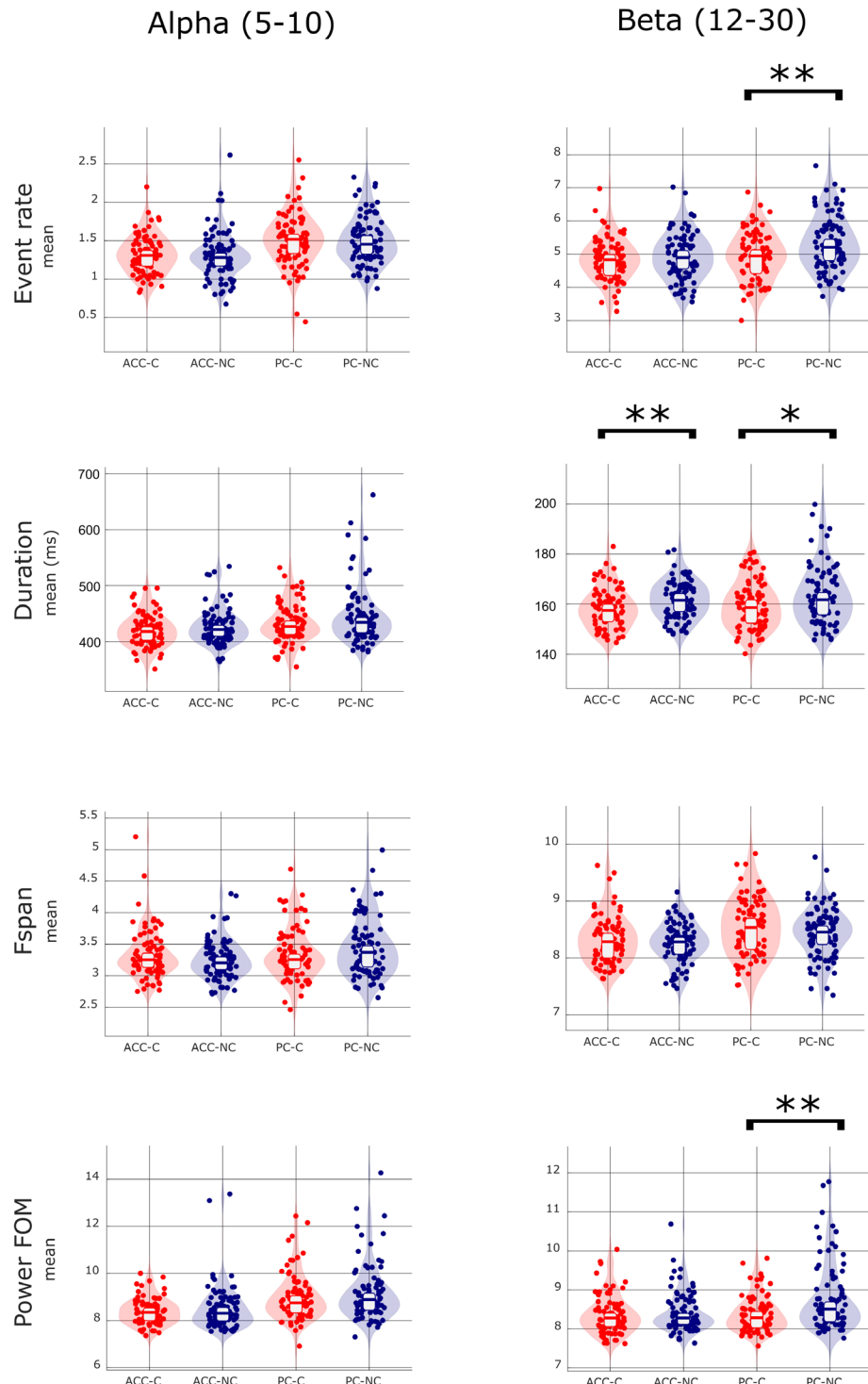


**Fig. 5.** Mean and distribution of event features for AD converters (CN) and non-converters (NC) in alpha [5–10] Hz and beta [12–30] Hz frequency bands. T-test statistically significant  $p$ -values ( $p < 0.05$ ) after BH correction are marked with the asterisk (\*\*). Statistical tendency ( $p < 0.1$ ) are marked with the asterisk (\*).

**Table 2.** Statistical comparison of event features averaged for CONV and NOCONV groups in low-alpha [5–10] Hz and beta [12–30] Hz frequency bands and x6 FOM.

Freq.	ROI	Feature	CONV	NOCONV	t Stat	p	Cohen d
			Mean ± SD	Mean ± SD			
Low-alpha [5–10] Hz	ACC	Ev.rate	1.32 ± 0.25	1.30 ± 0.31	t(165) = 0.41	0.343	-0.12
		Duration	419.6 ± 28.9	426.2 ± 32.3	t(168) = -1.40	0.918	0.17
		Fspan	3.33 ± 0.39	3.24 ± 0.30	t(168) = 1.67	0.048	-0.26
		Pow.FOM	8.39 ± 0.56	8.51 ± 0.94	t(144) = -1.02	0.844	0.04
	PC	Ev.rate	1.50 ± 0.34	1.50 ± 0.31	t(162) = 0.13	0.450	-0.08
		Duration	432.5 ± 34.4	445.4 ± 51.4	t(153) = -1.93	0.972	0.18
		Fspan	3.33 ± 0.41	3.44 ± 0.45	t(168) = -1.59	0.943	0.27
		Pow.FOM	8.99 ± 1.00	9.19 ± 1.19	t(166) = -1.17	0.878	0.16
Beta [12–30] Hz	ACC	Ev.rate	4.84 ± 0.63	4.92 ± 0.69	t(168) = -0.77	0.222	0.11
		Duration	158.3 ± 8.0	161.7 ± 7.3	t(164) = -2.93	0.002**	0.48
		Fspan	8.32 ± 0.41	8.26 ± 0.36	t(161) = 1.01	0.844	-0.05
		Pow.FOM	8.38 ± 0.51	8.43 ± 0.51	t(167) = -0.63	0.266	0.09
	PC	Ev.rate	4.94 ± 0.72	5.31 ± 0.82	t(167) = -3.10	0.001**	0.44
		Duration	159.6 ± 9.4	163.3 ± 11.5	t(168) = -2.25	0.013*	0.28
		Fspan	8.54 ± 0.50	8.44 ± 0.43	t(161) = 1.42	0.921	-0.18
		Pow.FOM	8.39 ± 0.46	8.78 ± 0.86	t(168) = -3.69	0.000**	0.50

An unpaired t-test for independent samples was applied. Significant differences after BH correction ( $p < 0.05$ ) are marked with the asterisk (\*\*). Statistical tendency ( $p < 0.1$ ) are marked with the asterisk (\*).

Although peak frequency was not a primary focus of our analysis, exploratory comparisons revealed no significant group differences between CONV and NOCONV (see Supplementary Fig. S7).

The fact that our method allows us to explain differences in beta band, but not in alpha band, could reflect the method's sensitivity in the alpha band. Indeed, as shown in Figure 4, in this subject sample, individual alpha event features are not a strong predictor of averaged alpha power (see also Supplementary Tables S1 and S2 for analysis of other power thresholds) and the slowing effects in the alpha band may instead be due to a combination of transient event features and/or more stationary properties of the signal.

To investigate the further predictive potential of resting-state beta event features as a biomarker for conversion from MCI to AD, we examined the association between beta event rate, duration, and maximum power and the probability of AD conversion within a 2.5-year time frame (see Fig. 6A). The probability of conversion was calculated from a logistic regression (see Methods section 2.5). Consistent with the pooled results in Figure 5, lower beta event rates, shorter duration, and reduced event power are linearly associated with an increased probability of conversion. MCI subjects with fewer than 4.92 events in 4 s of resting-state data have 1.79 (95% CI [1.1, 3.0]) times greater odds of converting to AD ( $R^2_{Nag} = .10$ ,  $p\text{-value} = .024$ ). Those with event duration less than 159 ms have 1.06 (95% CI [1.0, 1.1]) times greater odds of AD conversion ( $R^2_{Nag} = .06$ ,

$p\text{-value} = .008$ ), and subjects whose events have maxima power (calculated as factors of median power) less than 8.41 have 2.01 (95% CI [1.15, 3.76]) times greater odds of AD conversion ( $R^2_{Nag} = .05$ ,  $p\text{-value} = .019$ ).

Further examination of the relationship between beta event features and cognitive performance showed that, in the CONV group, a lower rate of beta events and lower power beta events were linearly associated with greater cognitive decline (Fig. 6B, lower Cognitive Performance Index values, see Methods section 2.5 Statistical Analysis) ( $\beta = .26$ ,  $R^2 = .07$ ,  $p\text{-value} = .016$  for number of events;  $\beta = .31$ ,  $R^2 = .10$ ,  $p\text{-value} = .0041$  for maxima power). These relationships did not emerge for duration, nor appear in NOCONVs, suggesting beta event features and particularly beta event power ( $p\text{-value} = 0.0041$ ) are predictive of cognitive decline only in MCI patients that will convert to AD within 2.5 years.

#### 4. DISCUSSION

Resting-state networks reflect intrinsic neural dynamics without behavioral confounds, providing non-invasive, reliable (Garcés et al., 2016), and sensitive biomarkers to examine human brain physiology associated with AD (Bruña et al., 2023; Hsiao et al., 2013; Ishii et al., 2017; López et al., 2020; López-Sanz et al., 2016). Oscillatory slowing has been associated with AD conversion based on PSD analysis that relies on signal averaging. Our study shows for the first time that in non-averaged data, resting-state alpha and beta oscillations from ACC and

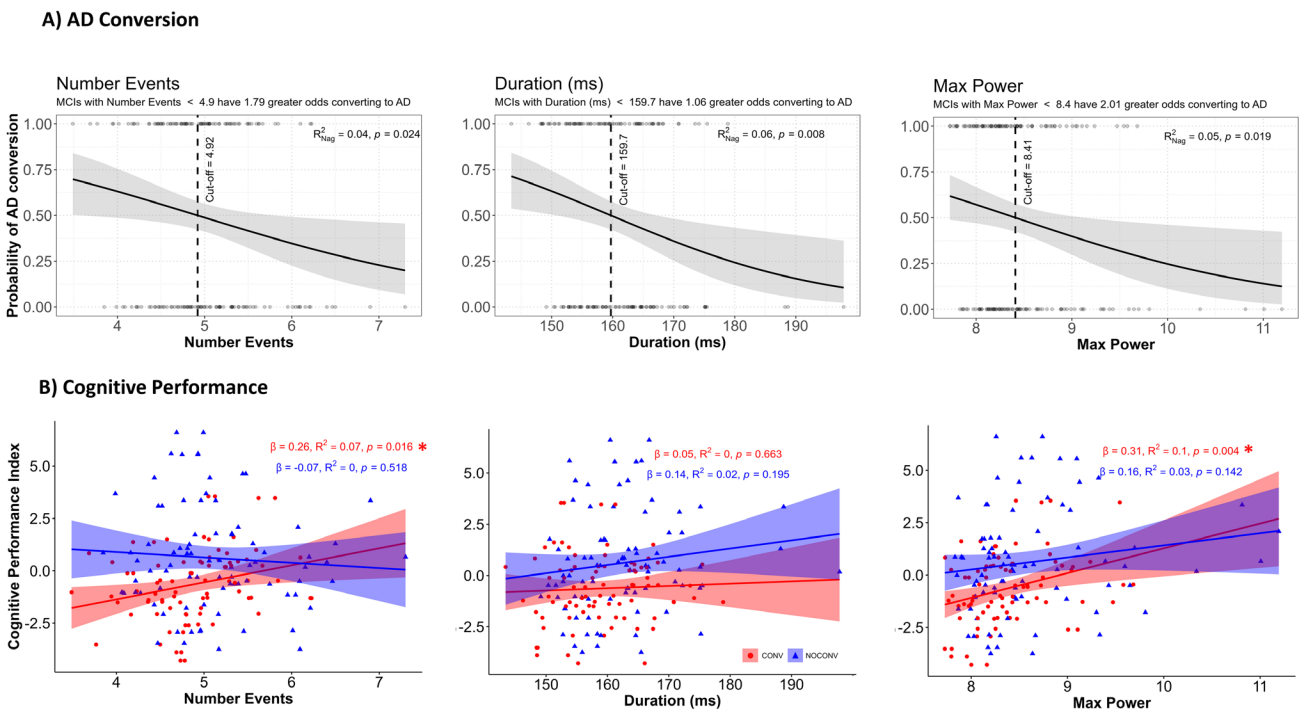


**Fig. 6.** Diminished expression of beta event features in ACC and PC (number of events, duration, maxima power) is associated with greater odds of future AD conversion, and reduced cognitive performance. (A) Logistic regression between beta event features and AD conversion within 2.5 years. (B) Linear regression between beta event features and Cognitive Performance Index separated by CONV (red) and NOCONV (blue).

PC are composed of transient high-power events. To explore how transient high-power events relate to findings of slowing in PSD, we studied their properties in a sample of individuals diagnosed as MCI and characterized novel features of transient high-power events that distinguish patients who later convert or do not convert to AD (i.e., CONV and NOCONV, respectively). Our analysis reveals a consistent pattern of a lower number of transient 12–30 Hz beta events, duration, and power for CONV compared with NOCONV in PC, with the duration effect also occurring in AC. This diminished beta event expression in ACC and PC was associated with increased odds of future AD conversion and decreased cognitive performance in the CONV group. It is well known that PC and ACC are part of the default mode network, which has decreased metabolism in the early stages of the disease (Greicius et al., 2004) and it is closely involved with episodic memory processing (Liu et al., 2022). Our finding of reduced event activation in CONV is predominantly found in precuneus, an ROI typically associated with deposition of amyloid- $\beta$  in the early stages of the AD continuum (Forsberg et al., 2008).

Overall, our results lay the foundation for further examination of beta event features as a novel biomarker for early AD diagnosis and possible neurobiological measures of the effectiveness of preventative interventions. A

more fine-grained description of slowing in unaveraged MEG data may also bring us closer to understanding the underlying neural mechanisms, and a more direct link to hyperexcitability as observed in animal models (Maestú et al., 2021; Zott et al., 2019), ultimately guiding new therapeutics in humans.

#### 4.1. Consistency with prior studies examining beta, aging, and cognitive control

Reductions in beta event expression yielded a lower PSD in the beta band [12–30] Hz averaged across trials, giving further insight into the underpinning of oscillatory slowing in AD (Bruña et al., 2023; Dauwels et al., 2011; Jelic et al., 2000). This trend is also consistent with a critical shift in beta activity at approximately 60 years of age in healthy patients (Brady et al., 2020; Power & Bardouille, 2021). Following this inflection point, resting-state relative source power, as well as beta event characteristics such as event rate, peak frequency, duration, peak power, etc., progressively begins to decline with age (Brady & Bardouille, 2022). Other studies have shown that averaged M/EEG spectral activity in the beta frequency range (13–30) Hz is a more powerful predictor of MCI-to-AD conversion than activity in other frequency bands, including in the slow alpha frequency range (Gaubert et al., 2025; Poil et al., 2013). Thus, transient

beta event features may be key factors in delineating differences and tracking the neurophysiology of healthy and pathological aging.

We found that reductions in beta event features were associated with global cognitive decline, as measured by an index based on a battery of neuropsychological tests. However, this effect is only significant in the CONV group. MCI patients who convert to AD 2.5 years later seem to be more reliant on beta event expression for cognitive robustness.

Several studies have shown that beta events throughout the cortex are a signature of inhibitory control. In sensory cortex, beta event expression can be manipulated with attention (increasing in non-attentive states), and an increase in beta event rates is associated with a decrease in perceptual salience (Shin et al., 2017), a process predicted to be mediated by an increase in inhibitory neuron activity (Law et al., 2022). In motor cortex, increased beta event expression is associated with inhibited motor control and Parkinson's disease (Yu et al., 2021), and in frontal cortex beta events are a signature of stopping of movement and long-term memory retrieval (Schmidt et al., 2019; Wessel, 2020). Conversely, reduction in beta event rates in frontal cortex has been explicitly linked to encoding and decoding in working memory processes, where they have been suggested as a mechanism for volitional control and memory content reactivation (Lundqvist et al., 2016, 2018; Spitzer & Haegens, 2017). Likewise, decreased posterior parietal beta oscillatory activity predicts episodic memory formation and retrieval (Griffiths et al., 2021a; Nyhus, 2018), and is correlated with enhanced memory performance (Griffiths et al., 2021b). Transcranial stimulation of the prefrontal cortex at beta (18 Hz) has been found to induce memory encoding impairments (Hanslmayr et al., 2014), and during posterior parietal cortex stimulation, lower prestimulus beta power predicts higher phosphene ratings, reflecting increased neural excitability (Samaha et al., 2017).

The consistent relationship between beta event expression and inhibitory control in these myriad studies (Lundqvist et al., 2024) suggests that the ability to modulate beta events according to task demands is necessary for optimal function, and that the diminished resting-state beta event expression and associated cognitive decline observed in the PC in CONV in our study may be directly related to lack of inhibitory cognitive control.

#### 4.2. Why are differences in alpha bursts not present?

Despite the observation of significant across group differences in alpha band in the average PSD (Fig. 2), we did not find a significant relationship between transient [5–10] Hz alpha event features and averaged power, nor

did we find a difference in event features between MCI patients who will convert to AD and those who will not, which is consistent with previous longitudinal studies of AD progression (Gaubert et al., 2025; Poil et al., 2013). This was true for several event detection thresholds (see Supplementary Fig. S4; Supplementary Tables S1 and S2).

Since we did not find a relationship between spectral events in the lower 5–10 Hz alpha band and averaged alpha power in our sample, we did not examine the relationship with cognitive performance. In terms of components of slowing, other studies have found a relationship between bursts of slow activity (1–6 Hz) age and cognition in healthy adults, where older subjects and lower cognitive performance participants exhibited longer and slower events (Power et al., 2024).

The lack of alpha event effects in our sample could reflect the sensitivity limitations of the spectral event detection method or indicate that, although the alpha band contains transient components, the differences between the two groups involve a combination of transient feature or more stationary features than transient ones. A slowed occipital alpha rhythm is a common biomarker of several neurological or psychiatric disorders (Hughes & Crunelli, 2005; Samson-Dollfus et al., 1997). According to the “thalamo-cortical hypothesis” (Klimesch et al., 2007; S. M. Sherman, 2001), slow cortical rhythms could be generated by TC cells in tonic, single spike, firing, or in arrhythmic bursting mode. Hughes and Crunelli (2005) argued that a slowing effect when shifting from alpha to theta waves could arise from the hyperpolarization of the thalamo-cortical neuron population, resulting in a deceleration of high-threshold bursting (HT) in individual cells, which could translate to a shift from bursty alpha to more continuous slower theta range oscillations. Thus, in this cognitively impaired population, while we still detect some alpha bursting, Alzheimer's disease-related mechanisms may be disrupting thalamo-cortical connections (Eustache et al., 2016) and slowing the thalamic bursting activity, making it more stationary.

In the early stages of AD continuum, even before a mild cognitive impairment diagnosis, alpha disruption is a marker of cognitive decline (Babiloni et al., 2010; Bruña et al., 2023; Huang et al., 2000; López et al., 2020; López-Sanz et al., 2016). Still, when patients reach a more advanced stage of the disease, as it is mild cognitive impairment, beta band is more discriminant between AD converters and non-converters (Gaubert et al., 2025; Poil et al., 2013; Pusil, Dimitriadis, et al., 2019). Consequently, when measured in MCIs, the spectral events method may not be sensitive to this transient-to-stationary shift in the alpha [5–10] Hz frequency band but can detect differences in the beta [12–30] Hz band.

#### 4.3. 1/f aperiodic activity and the thresholding dilemma

In recent years, there has been a surge of new techniques to improve the sensitivity of high-power event detection by removing the 1/f aperiodic component of the spectrum (Brady & Bardouille, 2022; Seymour et al., 2022; Szul et al., 2023). Our study focuses on very high-power transient events, defined as local power maxima exceeding a threshold of  $6 \times$  the median power at each frequency (Shin et al., 2017). While results computed with the SpectralEvents algorithm remain largely consistent after removing the aperiodic component (see Supplementary Figs. S2 and S3), alternative thresholding techniques may better capture the diversity of spectral event features. A lower variability in detected events could limit the proportion of variance explained in both averaged power and behavioral correlations. Future work may benefit from exploring thresholding approaches that are more sensitive to a broader range of transient dynamics, potentially improving interpretability and  $R^2$  correlations values between beta event features and other measures (e.g., Fig. 6).

#### 4.4. A mechanistic link between reduced beta event expression and hyperexcitability in CONV

Animal studies have suggested A  $\beta$ -induced changes in E/I balance are a mechanism for hyperexcitability and cognitive decline in Alzheimer's disease (Maestú et al., 2021). This notion has been supported by several computational neural modeling frameworks examining causal links between disease processes and increased neuron firing rates (Alexandersen et al., 2023; Cabral et al., 2014; de Haan et al., 2017; Hutt et al., 2023; Nakagawa et al., 2014; Stefanovski et al., 2019; Zimmermann et al., 2018), albeit without explicit consideration of the biophysical generators of MEG current sources or of beta frequency oscillations.

Modeling work by our group, specifically designed to interpret the detailed cell and circuit origin of localized MEG (and EEG) current source signals (Neymotin et al., 2020), provides a potential mechanistic hypothesis linking beta event expression to cortical excitability in CONV.

Specifically, our prior modeling and cross-species empirical studies suggested neocortical beta events are generated by bursts of exogenous thalamocortical drive that targets excitatory synapses on the proximal and distal dendrites of pyramidal neurons in deep and superficial neocortical layers, such that the distal drive is stronger and lasts a beta period (i.e.,  $\approx 50$  ms) (Jones et al., 2009; M. A. Sherman et al., 2016). This thalamic burst drive induces current flow in pyramidal neuron dendrites that generate MEG beta event waveform characteristics con-

sistent with those observed experimentally in sensory, motor, and frontal cortices (Bonaiuto et al., 2021; M. A. Sherman et al., 2016), and when occurring rhythmically can produce multiple beta cycles and/or a complex of alpha and beta activities (Jones et al., 2009). Follow-up studies predicted further that the thalamic drive inducing a beta event also activates inhibitory neurons in supragranular layers, providing a causal mechanism for beta-associated inhibitory control (Law et al., 2022; Shin et al., 2017). Together with our current findings that CONV has reduced beta expression (namely lower event rates, power, and duration), these prior studies open new framework to test in the AD continuum: CONV would have a reduction in thalamocortical burst drive to cortex, which in turn recruits less cortical inhibitory neuron activity leading to hyperexcitability. This interpretation, based on cross-species modeling and indirect evidence, should be viewed as a working hypothesis for future computational simulations and tested in animal studies.

Such a decrease in inhibitory activity may also align with animal studies reporting diminished GABAergic terminals on cortical neurons near amyloid plaques, in addition to the toxic effects of amyloid oligomers on inhibitory terminals (Alexandersen et al., 2023; Garcia-Marin et al., 2009), particularly in PC which exhibits A  $\beta$  deposition in the early stages of AD. The predicted reduction in thalamic bursting is also synergistic with studies showing thalamic atrophy and reduced inhibitory thalamic tone (Abuhassan et al., 2014; Forno et al., 2023), as inhibition from the thalamic reticular nucleus is known to be a driver of rebound bursting mechanisms in thalamic relay cells (Destexhe & Sejnowski, 2002). Moreover, decreases in thalamocortical drive are consistent with theories of thalamocortical dysrhythmia (Llinás et al., 1999) and could contribute to loss of cortical signal complexity and biophysical heterogeneity (Szul et al., 2023) occurring with the disease and thought to be an important homeostatic control mechanism capable of bolstering the network's resilience to perturbations, such as the toxic effects of amyloid (Dauwels et al., 2011; Hutt et al., 2023).

#### DATA AND CODE AVAILABILITY

Code to perform analyses is available at: <https://github.com/jonescompneurolab/SpectralEvents>. Data will be made available on request.

#### AUTHOR CONTRIBUTIONS

D.S.-B., G.S., and R.B.: methodology, software, analysis, visualization, original draft. D.W.Z., J.C., B.P.C., E.P., M.E.L., R.B., F.M., and S.R.J.: conceptualization, methodology, review, and editing.

## FUNDING

This work was supported by funds from NIH and the Collaborative Research in Computational Neuroscience (CRCNS) under the project - 1R01AG076227-01 “Interpreting MEG Biomarkers of Alzheimer’s Progression with Human Neocortical Neurosolver”. Project PCI2021-122069-2A funded by MCIN/AEI/10.13039/501100011033 and by the European Union “NextGenerationEU/PRTR”. UCM-Santander grants for PhD students, provided additional economical support to main author. Support for S.R.J. and D.W.Z. was also provided by National Institutes of Health grant RF1MH130415.

## DECLARATION OF COMPETING INTEREST

The authors declare no competing financial interests.

## SUPPLEMENTARY MATERIALS

Supplementary material for this article is available with the online version here: <https://doi.org/10.1162/IMAG.a.69>.

## REFERENCES

- Abuhassan, K., Coyle, D., & Maguire, L. (2014). Compensating for thalamocortical synaptic loss in Alzheimer’s disease. *Front Comput Neurosci*, 8, 65. <https://doi.org/10.1007/s10827-013-0462-8>
- Agrell, B., & Dehlin, O. (1998). The clock-drawing test. *Age Ageing*, 27(3), 399–404. <https://doi.org/10.1093/ageing/27.3.399>
- Alexandersen, C. G., de Haan, W., Bick, C., & Goriely, A. (2023). A multi-scale model explains oscillatory slowing and neuronal hyperactivity in Alzheimer’s disease. *J R Soc Interface*, 20(198), 20220607. <https://doi.org/10.1098/rsif.2022.0607>
- Algina, J., Keselman, H. J., & Penfield, R. D. (2005). An alternative to Cohen’s standardized mean difference effect size: A robust parameter and confidence interval in the two independent groups case. *Psychol Methods*, 10(3), 317–328. <https://doi.org/10.1037/1082-989x.10.3.317>
- Babiloni, C., Binetti, G., Cassetta, E., Cerbonescu, D., Dal Forno, G., Del Percio, C., Ferreri, F., Ferri, R., Lanuzza, B., Miniussi, C., Moretti, D. V., Nobili, F., Pascual-Marqui, R. D., Rodriguez, G., Romani, G. L., Salinari, S., Tecchio, F., Vitali, P., Zanetti, O., ... Rossini, P. M. (2004). Mapping distributed sources of cortical rhythms in mild Alzheimer’s disease. a multicentric EEG study. *Neuroimage*, 22(1), 57–67. <https://doi.org/10.1016/j.neuroimage.2003.09.028>
- Babiloni, C., Frisoni, G. B., Pievani, M., Vecchio, F., Lizio, R., Buttiglione, M., Geroldi, C., Fracassi, C., Eusebi, F., Ferri, R., & Rossini, P. M. (2009). Hippocampal volume and cortical sources of EEG alpha rhythms in mild cognitive impairment and Alzheimer disease. *Neuroimage*, 44(1), 123–135. <https://doi.org/10.1016/j.neuroimage.2008.08.005>
- Babiloni, C., Visser, P. J., Frisoni, G., De Deyn, P. P., Bresciani, L., Jelic, V., Nagels, G., Rodriguez, G., Rossini, P. M., Vecchio, F., Colombo, D., Verhey, F., Wahlund, L.-O., & Nobili, F. (2010). Cortical sources of resting EEG rhythms in mild cognitive impairment and subjective memory complaint. *Neurobiol Aging*, 31(10), 1787–1798. <https://doi.org/10.1016/j.neurobiolaging.2008.09.020>
- Bang, J., Spina, S., & Miller, B. L. (2015). Frontotemporal dementia. *Lancet*, 386(10004), 1672–1682. [https://doi.org/10.1016/s0140-6736\(15\)00461-4](https://doi.org/10.1016/s0140-6736(15)00461-4)
- Benjamini, Y., & Hochberg, Y. (1995). Controlling the false discovery rate: A practical and powerful approach to multiple testing. *J R Stat Soc, Ser B*, 57(1), 289–300. <https://doi.org/10.1111/j.2517-6161.1995.tb02031.x>
- Benton, A. L., Hamsher, K. d. S., & Sivan, A. B. (1994). *Multilingual aphasia examination* (3rd). Psychological Assessment Resources.
- Bonaiuto, J. J., Little, S., Neymotin, S. A., Jones, S. R., Barnes, G. R., & Bestmann, S. (2021). Laminar dynamics of high amplitude beta bursts in human motor cortex. *Neuroimage*, 242, 118479. <https://doi.org/10.1016/j.neuroimage.2021.118479>
- Bowie, C. R., & Harvey, P. D. (2006). Administration and interpretation of the trail making test. *Nature protocols*, 1(5), 2277–2281. <https://doi.org/10.1038/nprot.2006.390>
- Brady, B., & Bardouille, T. (2022). Periodic/Aperiodic parameterization of transient oscillations (PAPTO)—Implications for healthy ageing. *Neuroimage*, 251, 118974. <https://doi.org/10.1016/j.neuroimage.2020.117245>
- Brady, B., Power, L., & Bardouille, T. (2020). Age-related trends in neuromagnetic transient beta burst characteristics during a sensorimotor task and rest in the Cam-CAN open-access dataset. *Neuroimage*, 222, 117245. <https://doi.org/10.1016/j.neuroimage.2021.118670>
- Bruña, R., López-Sanz, D., Maestú, F., Cohen, A. D., Baigic, A., Huppert, T., Kim, T., Roush, R. E., Snitz, B., & Becker, J. T. (2023). MEG oscillatory slowing in cognitive impairment is associated with the presence of subjective cognitive decline. *Clin EEG Neurosci*, 54(1), 73–81. <https://doi.org/10.1016/j.clinph.2019.11.023>
- Cabral, J., Luckhoo, H., Woolrich, M., Joensson, M., Mohseni, H., Baker, A., Kringelbach, M. L., & Deco, G. (2014). Exploring mechanisms of spontaneous functional connectivity in MEG: How delayed network interactions lead to structured amplitude envelopes of band-pass filtered oscillations. *Neuroimage*, 90, 423–435. <https://doi.org/10.1016/j.neuroimage.2013.11.047>
- Cho, H., Choi, J. Y., Hwang, M. S., Kim, Y. J., Lee, H. M., Lee, H. S., Lee, J. H., Ryu, Y. H., Lee, M. S., & Lyoo, C. H. (2016). In vivo cortical spreading pattern of tau and amyloid in the Alzheimer disease spectrum. *Ann Neurol*, 80(2), 247–258. <https://doi.org/10.1002/ana.24711>
- da Silva, F. L. (2013). EEG and MEG: Relevance to neuroscience. *Neuron*, 80(5), 1112–1128. <https://doi.org/10.1016/j.neuron.2013.10.017>
- Dauwels, J., Srinivasan, K., Ramasubba Reddy, M., Musha, T., Vialatte, F.-B., Latchoumane, C., Jeong, J., & Cichocki, A. (2011). Slowing and loss of complexity in Alzheimer’s EEG: Two sides of the same coin? *Int J Alzheimers Dis*, 2011, 539621. <https://doi.org/10.4061/2011/539621>
- de Haan, W., van Straaten, E. C. W., Gouw, A. A., & Stam, C. J. (2017). Altering neuronal excitability to preserve network connectivity in a computational model of Alzheimer’s disease. *PLoS Comput Biol*, 13(9), e1005707. <https://doi.org/10.1371/journal.pcbi.1005707>
- Destexhe, A., & Sejnowski, T. J. (2002). The initiation of bursts in thalamic neurons and the cortical control of thalamic sensitivity. *Philos Trans R Soc B Biol Sci*,

- 357(1428), 1649–1657. <https://doi.org/10.1098/rstb.2002.1154>
- Eustache, P., Nemmi, F., Saint-Aubert, L., Pariente, J., & Péran, P. (2016). Multimodal magnetic resonance imaging in Alzheimer's disease patients at prodromal stage. *J Alzheimers Dis*, 50(4), 1035–1050. <https://doi.org/10.1111/ejn.15613/v2/response1>
- Forno, G., Saranathan, M., Contador, J., Guillen, N., Falgas, N., Tort-Merino, A., Balasa, M., Sanchez-Valle, R., Hornberger, M., & Lladó, A. (2023). Thalamic nuclei changes in early and late onset Alzheimer's disease. *Curr Res Neurobiol*, 4, 100084. <https://doi.org/10.1016/j.crneur.2023.100084>
- Forsberg, A., Engler, H., Almkvist, O., Blomquist, G., Hagman, G., Wall, A., Ringheim, A., Långström, B., & Nordberg, A. (2008). Pet imaging of amyloid deposition in patients with mild cognitive impairment. *Neurobiol Aging*, 29(10), 1456–1465. <https://doi.org/10.1016/j.neurobiolaging.2007.03.029>
- Garcés, P., Martín-Buro, M. C., & Maestú, F. (2016). Quantifying the test-retest reliability of magnetoencephalography resting-state functional connectivity. *Brain Connect*, 6(6), 448–460. <https://doi.org/10.1089/brain.2015.0416>
- Garcia-Marin, V., Blazquez-Llorca, L., Rodriguez, J.-R., Boluda, S., Muntane, G., Ferrer, I., & Defelipe, J. (2009). Diminished perisomatic GABAergic terminals on cortical neurons adjacent to amyloid plaques. *Front Neuroanat*, 3, 28. <https://doi.org/10.3389/neuro.05.028.2009>
- Gaubert, S., Garces, P., Hipp, J., Bruña, R., Lopéz, M. E., Maestú, F., Vaghari, D., Henson, R., Paquet, C., & Engemann, D.-A. (2025). Exploring the neuromagnetic signatures of cognitive decline from mild cognitive impairment to Alzheimer's disease dementia. *EBioMedicine*, 114, 105659. <https://doi.org/10.1016/j.ebiom.2025.105659>
- Greicius, M. D., Srivastava, G., Reiss, A. L., & Menon, V. (2004). Default mode network activity distinguishes Alzheimer's disease from healthy aging: Evidence from functional MRI. *Proc Natl Acad Sci USA*, 101(13), 4637–4642. <https://doi.org/10.1073/pnas.0308627101>
- Griffiths, B. J., Martín-Buro, M. C., Staresina, B. P., & Hanslmayr, S. (2021a). Disentangling neocortical alpha/beta and hippocampal theta/gamma oscillations in human episodic memory formation. *Neuroimage*, 242, 118454. <https://doi.org/10.1016/j.neuroimage.2021.118454>
- Griffiths, B. J., Martín-Buro, M. C., Staresina, B. P., Hanslmayr, S., & Staudigl, T. (2021b). Alpha/beta power decreases during episodic memory formation predict the magnitude of alpha/beta power decreases during subsequent retrieval. *Neuropsychologia*, 153, 107755. <https://doi.org/10.1016/j.neuropsychologia.2021.107755>
- Hämäläinen, M. S., & Ilmoniemi, R. J. (1994). Interpreting magnetic fields of the brain: Minimum norm estimates. *Med Biol Eng Comput*, 32(1), 35–42. <https://doi.org/10.1007/bf02512476>
- Hampel, H., Hardy, J., Blennow, K., Chen, C.-C., Perry, G., Kim, S.-H., Villemagne, V. L., Aisen, P., Vendruscolo, M., Iwatsubo, T., Masters, C. L., Cho, S. H., Vergallo, A., Baig, S., Kiddle, S. J., Baird, A. L., Potashman, M., Dean, R. A., Khachaturian, Z., & Snyder, H. M. (2021). The amyloid-pathway in Alzheimer's disease. *Mol Psychiatry*, 26(10), 5481–5503. <https://doi.org/10.1038/s41380-021-01249-0>
- Hanslmayr, S., Matuschek, J., & Fellner, M.-C. (2014). Entrainment of prefrontal beta oscillations induces an endogenous echo and impairs memory formation. *Curr Biol*, 24(8), 904–909. <https://doi.org/10.1016/j.cub.2014.03.007>
- Hoshi, H., Hirata, Y., Kobayashi, M., Sakamoto, Y., Fukasawa, K., Ichikawa, S., Poza, J., Rodríguez-González, V., Gómez, C., & Shigihara, Y. (2022). Distinctive effects of executive dysfunction and loss of learning/memory abilities on resting-state brain activity. *Sci Rep*, 12(1), 3459. <https://doi.org/10.1038/s41598-022-07202-7>
- Hsiao, F.-J., Wang, Y.-J., Yan, S.-H., Chen, W.-T., & Lin, Y.-Y. (2013). Altered oscillation and synchronization of default-mode network activity in mild Alzheimer's disease compared to mild cognitive impairment: An electrophysiological study. *PLoS One*, 8(7), e68792. <https://doi.org/10.1371/journal.pone.0068792>
- Huang, C., Wahlund, L., Dierks, T., Julin, P., Winblad, B., & Jelic, V. (2000). Discrimination of Alzheimer's disease and mild cognitive impairment by equivalent EEG sources: A cross-sectional and longitudinal study. *Clin Neurophysiol*, 111(11), 1961–1967. [https://doi.org/10.1016/s1388-2457\(00\)00454-5](https://doi.org/10.1016/s1388-2457(00)00454-5)
- Hughes, S. W., & Crunelli, V. (2005). Thalamic mechanisms of EEG alpha rhythms and their pathological implications. *Neuroscientist*, 11(4), 357–372. <https://doi.org/10.3580/071436>
- Hutt, A., Rich, S., Valiante, T. A., & Lefebvre, J. (2023). Intrinsic neural diversity quenches the dynamic volatility of neural networks. *Proc Natl Acad Sci USA*, 120(28), e2218841120. <https://doi.org/10.1073/pnas.2218841120>
- Ishii, R., Canuet, L., Aoki, Y., Hata, M., Iwase, M., Ikeda, S., Nishida, K., & Ikeda, M. (2017). Healthy and pathological brain aging: From the perspective of oscillations, functional connectivity, and signal complexity. *Neuropsychobiology*, 75(4), 151–161. <https://doi.org/10.1159/000486870>
- Jelic, V., Johansson, S. E., Almkvist, O., Shigeta, M., Julin, P., Nordberg, A., Winblad, B., & Wahlund, L. O. (2000). Quantitative electroencephalography in mild cognitive impairment: Longitudinal changes and possible prediction of Alzheimer's disease. *Neurobiol Aging*, 21(4), 533–540. [https://doi.org/10.1016/s0197-4580\(00\)00153-6](https://doi.org/10.1016/s0197-4580(00)00153-6)
- Jeong, J. (2004). EEG dynamics in patients with Alzheimer's disease. *Clin Neurophysiol*, 115(7), 1490–1505. [https://doi.org/10.1016/s1388-2457\(01\)00513-2](https://doi.org/10.1016/s1388-2457(01)00513-2)
- Jones, S. R. (2016). When brain rhythms aren't 'rhythmic': Implication for their mechanisms and meaning. *Curr Opin Neurobiol*, 40, 72–80. <https://doi.org/10.1016/j.conb.2016.06.010>
- Jones, S. R., Pritchett, D. L., Sikora, M. A., Stufflebeam, S. M., Härmäläinen, M., & Moore, C. I. (2009). Quantitative analysis and biophysically realistic neural modeling of the MEG mu rhythm: Rhythmogenesis and modulation of sensory-evoked responses. *J Neurophysiol*, 102(6), 3554–3572. <https://doi.org/10.1152/jn.00535.2009>
- Kaplan, E., Goodglass, H., & Weintraub, S. (1983). *The Boston naming test*. Lea Febiger.
- Kavanaugh, B. C., Fukuda, A. M., Gemelli, Z. T., Thorpe, R., Tirrell, E., Vigne, M., Jones, S. R., & Carpenter, L. L. (2023). Pre-treatment frontal beta events are associated with executive dysfunction improvement after repetitive transcranial magnetic stimulation for depression: A preliminary report. *J Psychiatr Res*, 168, 71–81. <https://doi.org/10.1016/j.bandc.2024.106164>
- Kavanaugh, B. C., Vigne, M. M., Tirrell, E., Acuff, W. L., Fukuda, A. M., Thorpe, R., Sherman, A., Jones, S. R., Carpenter, L. L., & Tyrka, A. R. (2024). Frontoparietal beta event characteristics are associated with early life stress

- and psychiatric symptoms in adults. *Brain Cogn*, 177, 106164. <https://doi.org/10.1016/j.bandc.2024.106164>
- Klimesch, W., Sauseng, P., & Hanslmayr, S. (2007). EEG alpha oscillations: The inhibition-timing hypothesis. *Brain Res Rev*, 53(1), 63–88. <https://doi.org/10.1016/j.neuroscience.2007.03.014>
- König, T., Prichep, L., Dierks, T., Hubl, D., Wahlund, L. O., John, E. R., & Jelic, V. (2005). Decreased EEG synchronization in Alzheimer's disease and mild cognitive impairment. *Neurobiol Aging*, 26(2), 165–171. <https://doi.org/10.1016/j.neurobiolaging.2004.03.008>
- Law, R. G., Pugliese, S., Shin, H., Sliva, D. D., Lee, S., Neymotin, S., Moore, C., & Jones, S. R. (2022). Thalamocortical mechanisms regulating the relationship between transient beta events and human tactile perception. *Cerebr Cortex*, 32(4), 668–688. <https://doi.org/10.1101/2021.04.16.440210>
- Liu, Y., Nour, M. M., Schuck, N. W., Behrens, T. E., & Dolan, R. J. (2022). Decoding cognition from spontaneous neural activity. *Nat Rev Neurosci*, 23(4), 204–214. <https://doi.org/10.1038/s41583-022-00570-z>
- Llinás, R. R., Ribary, U., Jeanmonod, D., Kronberg, E., & Mitra, P. P. (1999). Thalamocortical dysrhythmia: A neurological and neuropsychiatric syndrome characterized by magnetoencephalography. *Proc Natl Acad Sci USA*, 96(26), 15222–15227. <https://doi.org/10.1073/pnas.96.26.15222>
- López, M. E., Turrero, A., Cuesta, P., López-Sanz, D., Bruña, R., Marcos, A., Gil, P., Yus, M., Barabash, A., Cabranes, J. A., Maestú, F., & Fernández, A. (2016). Searching for primary predictors of conversion from mild cognitive impairment to Alzheimer's disease: A multivariate follow-up study. *J Alzheimers Dis*, 52(1), 133–143. <https://doi.org/10.3233/JAD-151034>
- López, M. E., Turrero, A., Cuesta, P., Rodríguez-Rojo, I. C., Barabash, A., Marcos, A., Maestú, F., & Fernández, A. (2020). A multivariate model of time to conversion from mild cognitive impairment to Alzheimer's disease. *Geroscience*, 42, 1715–1732. <https://doi.org/10.1002/alz.047537>
- López-Sanz, D., Bruña, R., Garcés, P., Camara, C., Serrano, N., Rodríguez-Rojo, I. C., Delgado, M. L., Montenegro, M., López-Higes, R., Yus, M., & Maestú, F. (2016). Alpha band disruption in the AD-continuum starts in the subjective cognitive decline stage: A MEG study. *Sci Rep*, 6, 37685. <https://doi.org/10.3389/fnagi.2017.00109>
- López-Sanz, D., Bruña, R., Garcés, P., Martín-Buro, M. C., Walter, S., Delgado, M. L., Montenegro, M., López Higes, R., Marcos, A., & Maestú, F. (2017). Functional connectivity disruption in subjective cognitive decline and mild cognitive impairment: A common pattern of alterations. *Front Aging Neurosci*, 9, 109. <https://doi.org/10.1142/s0129065717500411>
- Lundqvist, M., Herman, P., Warden, M. R., Brincat, S. L., & Miller, E. K. (2018). Gamma and beta bursts during working memory readout suggest roles in its volitional control. *Nat Commun*, 9(1), 1–12. <https://doi.org/10.1038/s41467-021-21151-1>
- Lundqvist, M., Miller, E. K., Nordmark, J., Liljefors, J., & Herman, P. (2024). Beta: Bursts of cognition. *Trends Cogn Sci*, 28(7), 662–676. <https://doi.org/10.1016/j.tics.2024.03.010>
- Lundqvist, M., Rose, J., Herman, P., Brincat, S. L., Buschman, T. J., & Miller, E. K. (2016). Gamma and beta bursts underlie working memory. *Neuron*, 90(1), 152–164. <https://doi.org/10.1016/j.neuron.2016.02.028>
- Maestú, F., de Haan, W., Busche, M. A., & DeFelipe, J. (2021). Neuronal excitation/inhibition imbalance: Core element of a translational perspective on Alzheimer pathophysiology. *Ageing Res Rev*, 69, 101372. <https://doi.org/10.1016/j.arr.2021.101372>
- Maris, E., & Oostenveld, R. (2007). Nonparametric statistical testing of EEG- and MEG-data. *J Neurosci Methods*, 164(1), 177–190. <https://doi.org/10.1016/j.jneumeth.2007.03.024>
- McKeon, S. D., Calabro, F., Thorpe, R. V., de la Fuente, A., Foran, W., Parr, A. C., Jones, S. R., & Luna, B. (2023). Age-related differences in transient gamma band activity during working memory maintenance through adolescence. *Neuroimage*, 274, 120112. <https://doi.org/10.1016/j.biopsych.2023.02.107>
- McKhann, G. M., Knopman, D. S., Chertkow, H., Hyman, B. T., Jack, C. R. J., Kawas, C. H., Klunk, W. E., Koroshetz, W. J., Manly, J. J., Mayeux, R., Mohs, R. C., Morris, J. C., Rossor, M. N., Scheltens, P., Carrillo, M. C., Thies, W., Weintraub, S., & Phelps, C. H. (2011). The diagnosis of dementia due to Alzheimer's disease: Recommendations from the national institute on aging-Alzheimer's association workgroups on diagnostic guidelines for Alzheimer's disease. *Alzheimers Dement*, 7(3), 263–269. <https://doi.org/10.1016/j.jalz.2011.03.005>
- Morris, A. T., Temereanca, S., Zandvakili, A., Thorpe, R., Sliva, D. D., Greenberg, B. D., Carpenter, L. L., Philip, N. S., & Jones, S. R. (2023). Fronto-central resting-state 15–29 Hz transient beta events change with therapeutic transcranial magnetic stimulation for posttraumatic stress disorder and major depressive disorder. *Sci Rep*, 13(1), 6366. <https://doi.org/10.1038/s41598-023-32801-3>
- Nakagawa, T. T., Woolrich, M., Luckhoo, H., Joensson, M., Mohseni, H., Kringselbach, M. L., Jirsa, V., & Deco, G. (2014). How delays matter in an oscillatory whole-brain spiking-neuron network model for MEG alpha-rhythms at rest. *Neuroimage*, 87, 383–394. <https://doi.org/10.1016/j.neuroimage.2013.11.009>
- Nakamura, A., Cuesta, P., Fernández, A., Arahata, Y., Iwata, K., Kuratsubo, I., Bundo, M., Hattori, H., Sakurai, T., Fukuda, K., Washimi, Y., Endo, H., Takeda, A., Diers, K., Bajo, R., Maestú, F., Ito, K., & Kato, T. (2018). Electromagnetic signatures of the preclinical and prodromal stages of Alzheimer's disease. *Brain*, 141(5), 1470–1485. <https://doi.org/10.1093/brain/awy044>
- Neymotin, S. A., Daniels, D. S., Caldwell, B., McDougal, R. A., Carnevale, N. T., Jas, M., Moore, C. I., Hines, M. L., Härmäläinen, M., & Jones, S. R. (2020). Human neocortical neurosolver (HNN), a new software tool for interpreting the cellular and network origin of human MEG/EEG data. *eLife*, 9, e51214. <https://doi.org/10.7554/elife.51214.sa2>
- Nyhus, E. (2018). Brain networks related to beta oscillatory activity during episodic memory retrieval. *J Cogn Neurosci*, 30(2), 174–187. [https://doi.org/10.1162/jocn\\_a\\_01194](https://doi.org/10.1162/jocn_a_01194)
- Oostenveld, R., Fries, P., Maris, E., & Schoffelen, J.-M. (2011). FieldTrip: Open source software for advanced analysis of MEG, EEG, and invasive electrophysiological data. *Comput Intell Neurosci*, 2011, 156869. <https://doi.org/10.1155/2011/156869>
- Poil, S.-S., de Haan, W., van der Flier, W. M., Mansvelder, H. D., Scheltens, P., & Linkenkaer-Hansen, K. (2013). Integrative EEG biomarkers predict progression to Alzheimer's disease at the MCI stage. *Front Aging Neurosci*, 5, 58. <https://doi.org/10.3389/fnagi.2013.00058>
- Power, L., & Bardouille, T. (2021). Age-related trends in the cortical sources of transient beta bursts during a

- sensorimotor task and rest. *Neuroimage*, 245, 118670. <https://doi.org/10.1016/j.neuroimage.2021.118670>
- Power, L., Friedman, A., & Bardouille, T. (2024). Atypical paroxysmal slow cortical activity in healthy adults: Relationship to age and cognitive performance. *Neurobiol Aging*, 136, 44–57. <https://doi.org/10.1016/j.neurobiolaging.2024.01.009>
- Pusil, S., Dimitriadis, S. I., López, M. E., Pereda, E., & Maestú, F. (2019). Aberrant MEG multi-frequency phase temporal synchronization predicts conversion from mild cognitive impairment-to-Alzheimer's disease. *Neuroimage Clin*, 24, 101972. <https://doi.org/10.1016/j.neuroimage.2018.10.068>
- Pusil, S., López, M. E., Cuesta, P., Bruña, R., Pereda, E., & Maestú, F. (2019). Hypersynchronization in mild cognitive impairment: The 'x' model. *Brain*, 142(12), 3936–3950. <https://doi.org/10.1093/brain/awz320>
- Quinn, A. J., van Ede, F., Brookes, M. J., Heideman, S. G., Nowak, M., Seedat, Z. A., Vidaurre, D., Zich, C., Nobre, A. C., & Woolrich, M. W. (2019). Unpacking transient event dynamics in electrophysiological power spectra. *Brain Topogr*, 32(6), 1020–1034. <https://doi.org/10.1007/s10548-019-00745-5>
- Samaha, J., Gossseries, O., & Postle, B. R. (2017). Distinct oscillatory frequencies underlie excitability of human occipital and parietal cortex. *J Neurosci*, 37(11), 2824–2833. <https://doi.org/10.1523/jneurosci.3413-16.2017>
- Samson-Dollfus, D., Delapierre, G., Do Marcolino, C., & Blondeau, C. (1997). Normal and pathological changes in alpha rhythms. *Int J Psychophysiol*, 26(1–3), 395–409. [https://doi.org/10.1016/s0167-8760\(97\)00778-2](https://doi.org/10.1016/s0167-8760(97)00778-2)
- Schaefer, A., Kong, R., Gordon, E. M., Laumann, T. O., Zuo, X.-N., Holmes, A. J., Eickhoff, S. B., & Yeo, B. T. T. (2018). Local-Global parcellation of the human cerebral cortex from intrinsic functional connectivity MRI. *Cerebr Cortex*, 28(9), 3095–3114. <https://doi.org/10.1101/135632>
- Schmidt, R., Herrojo Ruiz, M., Kilavik, B. E., Lundqvist, M., Starr, P. A., & Aron, A. R. (2019). Beta oscillations in working memory, executive control of movement and thought, and sensorimotor function. *J Neurosci*, 39(42), 8231–8238. <https://doi.org/10.1515/9780773594647-009>
- Sepulcre, J., Grothe, M. J., d’Oleire Uquillas, F., Ortiz-Terán, L., Diez, I., Yang, H.-S., Jacobs, H. I. L., Hanseeuw, B. J., Li, Q., El-Fakhri, G., Sperling, R. A., & Johnson, K. A. (2018). Neurogenetic contributions to amyloid beta and tau spreading in the human cortex. *Nat Med*, 24(12), 1910–1918. <https://doi.org/10.1038/s41591-018-0206-4>
- Seymour, R. A., Alexander, N., & Maguire, E. A. (2022). Robust estimation of 1/f activity improves oscillatory burst detection. *Eur J Neurosci*, 56(10), 5836–5852. <https://doi.org/10.1111/ejn.15829>
- Sherman, M. A., Lee, S., Law, R., Haegens, S., Thorn, C. A., Hämäläinen, M. S., Moore, C. I., & Jones, S. R. (2016). Neural mechanisms of transient neocortical beta rhythms: Converging evidence from humans, computational modeling, monkeys, and mice. *Proc Natl Acad Sci USA*, 113(33), E4885–E4894. <https://doi.org/10.1073/pnas.1604135113>
- Sherman, S. M. (2001). Tonic and burst firing: Dual modes of thalamocortical relay. *Trends Neurosci*, 24(2), 122–126. [https://doi.org/10.1016/s0166-2236\(00\)01714-8](https://doi.org/10.1016/s0166-2236(00)01714-8)
- Shin, H., Law, R., Tsutsui, S., Moore, C. I., & Jones, S. R. (2017). The rate of transient beta frequency events predicts behavior across tasks and species. *eLife*, 6, e29086. <https://doi.org/10.7554/elife.29086.025>
- Spitzer, B., & Haegens, S. (2017). Beyond the status quo: A role for beta oscillations in endogenous content (Re)
- Activation. *eNeuro*, 4(4), ENEURO.0170-17.2017. <https://doi.org/10.1523/ENEURO.0170-17.2017>
- Stefanovski, L., Triebkorn, P., Spiegler, A., Diaz-Cortes, M.-A., Solodkin, A., Jirsa, V., McIntosh, A. R., Ritter, P., & Alzheimer’s Disease Neuroimaging Initiative. (2019). Linking molecular pathways and Large-Scale computational modeling to assess candidate disease mechanisms and pharmacodynamics in Alzheimer’s disease. *Front Comput Neurosci*, 13, 54. <https://doi.org/10.1002/trc.21230>
- Stoiljkovic, M., Kelley, C., Horvath, T. L., & Hajós, M. (2018). Neurophysiological signals as predictive translational biomarkers for Alzheimer’s disease treatment: Effects of donepezil on neuronal network oscillations in TgF344-AD rats. *Alzheimers Res Ther*, 10(1), 105. <https://doi.org/10.1186/s13195-018-0433-4>
- Szul, M. J., Papadopoulos, S., Alavizadeh, S., Daligaut, S., Schwartz, D., Mattout, J., & Bonaiuto, J. J. (2023). Diverse beta burst waveform motifs characterize movement-related cortical dynamics. *Progr Neurobiol*, 228, 102490. <https://doi.org/10.1016/j.pneurobio.2023.102490>
- Tadel, F., Baillet, S., Mosher, J. C., Pantazis, D., & Leahy, R. M. (2011). Brainstorm: A user-friendly application for MEG/EEG analysis. *Comput Intell Neurosci*, 2011, 879716. <https://doi.org/10.1155/2011/879716>
- Taulu, S., & Hari, R. (2009). Removal of magnetoencephalographic artifacts with temporal signal-space separation: Demonstration with single-trial auditory-evoked responses. *Hum Brain Mapp*, 30(5), 1524–1534. <https://doi.org/10.1002/hbm.20627>
- Tekin, S., Mega, M. S., Masterman, D. M., Chow, T., Garakian, J., Vinters, H. V., & Cummings, J. L. (2001). Orbitofrontal and anterior cingulate cortex neurofibrillary tangle burden is associated with agitation in Alzheimer disease. *Ann Neurol*, 49(3), 355–361. <https://doi.org/10.1002/ana.72.abs>
- Tröndle, M., Popov, T., Pedroni, A., Pfeiffer, C., Bara czuk-Turska, Z., & Langer, N. (2023). Decomposing age effects in EEG alpha power. *Cortex*, 161, 116–144. <https://doi.org/10.7554/elife.77571>
- van Ede, F., Quinn, A. J., Woolrich, M. W., & Nobre, A. C. (2018). Neural oscillations: Sustained rhythms or transient Burst-Events? *Trends Neurosci*, 41(7), 415–417. <https://doi.org/10.1016/j.tins.2018.04.004>
- Wechsler, D. (1997). *Wechsler adult intelligence scale – third edition (waits-iii): Administration and scoring manual*. Psychological Corporation.
- Welch, P. (1967). The use of fast Fourier transform for the estimation of power spectra: A method based on time averaging over short, modified periodograms. *IEEE Trans Audio Electroacoust*, 15(2), 70–73. <https://doi.org/10.1109/tau.1969.1162040>
- Wessel, J. R. (2020). β-Bursts reveal the Trial-to-Trial dynamics of movement initiation and cancellation. *J Neurosci*, 40(2), 411–423. <https://doi.org/10.1523/jneurosci.1887-19.2019>
- Wiesman, A. I., Murman, D. L., Losh, R. A., Schantell, M., Christopher-Hayes, N. J., Johnson, H. J., Willett, M. P., Wolfson, S. L., Losh, K. L., Johnson, C. M., Griffith, E. H., Thompson, J. W., Eskildsen, S. F., Anazodo, U., Toledo, J. B., Sidiropoulos, C., MacDonald, T. J., Golomb, J., Gagnon, D., & Husamuldeen, H. (2022). Spatially resolved neural slowing predicts impairment and amyloid burden in Alzheimer’s disease. *Brain*, 145(6), 2177–2189. <https://doi.org/10.1093/brain/awac109>
- World Health Organization. (2017). Consultation on the development of the global dementia observatory, World Health Organization, Geneva, 5–6 July 2016: Meeting

- report (Accessed: October 19, 2023). <https://iris.who.int/bitstream/handle/10665/255552/WHO-MSD-MER-17.4-eng.pdf>
- Yu, Y., Sanabria, D. E., Wang, J., Hendrix, C. M., Zhang, J., Nebeck, S. D., Amundson, A. M., Busby, Z. B., Bauer, D. L., Johnson, M. D., Johnson, L. A., & Vitek, J. L. (2021). Parkinsonism alters beta burst dynamics across the basal Ganglia–Motor cortical network. *J Neurosci*, 41(10), 2274–2286. <https://doi.org/10.1152/jn.00388.2017>
- Zimmermann, J., Perry, A., Breakspear, M., Schirner, M., Sachdev, P., Wen, W., Kochan, N. A., Mapstone, M., Ritter, P., McIntosh, A. R., & Solodkin, A. (2018). Differentiation of Alzheimer's disease based on local and global parameters in personalized virtual brain models. *Neuroimage Clin*, 19, 240–251. <https://doi.org/10.1016/j.nicl.2018.04.017>
- Zott, B., Simon, M. M., Hong, W., Unger, F., Chen-Engerer, H.-J., Frosch, M. P., Sakmann, B., Walsh, D. M., & Konnerth, A. (2019). A vicious cycle of  $\beta$ -amyloid-dependent neuronal hyperactivation. *Science*, 365(6453), 559–565. <https://doi.org/10.1126/science.aay0198>